受入
81-5-289
高工研図書室

EUROPEAN ORGANIZATION FOR NUCLEAR RESEARCH

CERN-EP/81-35
16 April 1981

POLARIZATION EFFECTS FOR $W^{\pm}$ AND Z^0 PRODUCTION IN $\bar{p}p$ COLLISIONS

R. Kinnunen and J. Lindfors*)

CERN, Geneva, Switzerland

ABSTRACT

Polarization effects for the leptonic decays of $W^{\pm}$ and Z^0 are calculated and discussed in $\bar{p}p$ collisions with longitudinally polarized proton beams. Numerical examples are given for the CERN $\bar{p}p$ collider and Fermilab Tevatron.

Submitted to Nucl. Phys. B

*) Present address: Research Institute for Theoretical Physics, University of Helsinki, Helsinki, Finland.

1. INTRODUCTION

The production of the weak vector bosons, $W^{\pm}$ and Z^0, in high-energy $\bar{p}p$ and pp collisions can be expected to be strongly affected by the longitudinal polarization of the colliding hadrons. Because of the V-A structure of the theory the left-handed protons should produce a substantially larger number of W's than the right-handed protons. The investigation of the polarization effects for $W^{\pm}$ and Z^0 production will be of more than theoretical interest because of the realistic possibilities[1] of polarizing the high-energy proton beams with sufficient luminosities.

There already exist calculations on the polarization effects in the hadronic decays of $W^{\pm}$ by Haber and Kane[2] and Paige et al.[3]. In this work we study the effects of the longitudinal polarization of the incident proton for the leptonic decays of $W^{\pm}$ and Z^0 in $\bar{p}p$ collisions. Some results for leptonic decays have already been presented by Paige et al.[3] and Paige[4].

We calculate the cross-sections for $W^{\pm}$ and Z^0 in the standard SU(2) × U(1) model from the dominating Drell-Yan diagram, which is the procedure used previously by many authors[5]. The leading order logarithmic quantum chromodynamics (QCD) effect is also included in our calculations by using the non-scaling parton distribution functions. The higher order QCD corrections for $W^{\pm}$ and Z^0 production[6] are not expected to change essentially the polarization asymmetries as calculated from the basic Drell-Yan process and therefore they are not studied in this work. For the parton distribution functions in the longitudinally polarized proton we use the predictions of the SU(6) model[7]. Furthermore, we assume that the sea-quark component remains unpolarized.

We proceed as follows: In Section 2 we present the Drell-Yan process for longitudinally polarized partons; in Section 3 we calculate the cross-section for single-lepton production from $W^{\pm}$ and in Section 4 we calculate the cross-section for lepton-pair production from Z^0 in $\bar{p}p$ collisions with a longitudinally polarized proton beam. The effects of QCD corrections to polarization asymmetries are briefly discussed in Section 5 and finally the conclusions are given in Section 6.

2. DRELL-YAN PROCESS FOR POLARIZED PARTONS

We use the Drell-Yan model to calculate the cross-sections at the parton level. The Drell-Yan diagram for the annihilation of a quark and an antiquark to leptons is shown in Fig. 1a. The intermediate particle is $W^{\pm}$, Z^0, or γ. We use the notation where p_1 and p_2 denote the momenta and s_1 and s_2 the spin vectors of the quarks. Similarly, k_1 and k_2 are the momenta of the leptons and r_1 and r_2 their spin vectors. Then the momentum of the intermediate particle is given by $P = p_1 + p_2 = k_1 + k_2$. Using the general form $a + b\gamma_5$ for the vertices the amplitude for the process in Fig. 1a is

$$m = C\,\bar{v}(p_2,s_2)\gamma_\mu\left(a^q + b^q\gamma_5\right)u(p_1,s_1)\,\frac{g^{\mu\nu} - P^\mu P^\nu/M^2}{P^2 - M^2 + i\,\Gamma M}$$

$$\times\,\bar{u}(k_1,r_1)\gamma_\nu\left(a^\ell + b^\ell\gamma_5\right)v(k_2,r_2)\ . \qquad (1)$$

where M is the mass and Γ the width of the vector boson ($W^{\pm}$ or Z^0). We now let the quarks be in definite helicity states. Hence when taking the square of the amplitude we sum over the final spin states but take the helicity projection of the initial spins using the helicity operators

$$u(p_1,s_1)\bar{u}(p_1,s_1) = \frac{1 + h_1\gamma_5}{2}\,\not{p}_1$$

$$v(p_2,s_2)\bar{v}(p_2,s_2) = \frac{1 - h_2\gamma_5}{2}\,\not{p}_2\ ,$$

where h_1 is the helicity of the quark and h_2 that of the antiquark. Then we end up with the general form

$$\overline{|m|^2} = \frac{|C|^2}{16}\,\frac{1}{(P^2 - M^2)^2 + (\Gamma M)^2}$$

$$\times\,\mathrm{Tr}\left[\not{p}_2\gamma_\mu\not{p}_1\gamma_\alpha\left(A^q + B^q\gamma_5\right)(H_1 + H_2\gamma_5)\right]\cdot\mathrm{Tr}\left[\not{k}_1\gamma^\mu\not{k}_2\gamma^\alpha\left(A^\ell + B^\ell\gamma_5\right)\right]\ , \qquad (2)$$

which will be applied in the following for $W^{\pm}$, Z^0, and γ production. In the above we have used the definitions

$$H_1 = 1 - h_1h_2, \qquad H_2 = h_1 - h_2 ,$$

$$A^q = \left(a^q\right)^2 + \left(b^q\right)^2 , \qquad A^\ell = \left(a^\ell\right)^2 + \left(b^\ell\right)^2 ,$$

$$B^q = 2a^qb^q , \qquad B^\ell = 2a^\ell b^\ell .$$

In the SU(2) × U(1) model the vector and axial parts of the coupling constant have the following values:

for $W^\pm$:

$$C = \frac{e}{2\sqrt{2}\,\sin\theta_W} ,$$

$$a^q = a^\ell = 1 , \tag{3}$$

$$b^q = b^\ell = -1 ;$$

for Z^0:

$$C = \frac{e}{\sin\theta_W \cos\theta_W} ,$$

$$a^u = \tfrac{1}{4} - \tfrac{2}{3}\sin^2\theta_W , \qquad b^u = -\tfrac{1}{4} ,$$

$$a^d = -\tfrac{1}{4} + \tfrac{1}{3}\sin^2\theta_W , \qquad b^d = \tfrac{1}{4} , \tag{4}$$

$$a^\nu = \tfrac{1}{4} , \qquad b^\nu = -\tfrac{1}{4} ,$$

$$a^\ell = -\tfrac{1}{4} + \sin^2\theta_W , \qquad b^\ell = \tfrac{1}{4} ;$$

for γ:

$$C = eQ_q ,$$

$$a^q = a^\ell = 1 , \tag{5}$$

$$b^q = b^\ell = 0 ,$$

where Q_q is the quark charge. Using the experimental result $\sin^2\theta_W = 0.23$, we get the following numerical values for the mass and width of $W^\pm$ and Z^0:

$$M_W = \left(\frac{\pi\alpha}{G_F\sqrt{2}}\right)^{\frac{1}{2}} \frac{1}{\sin^2\theta_W} = 77.8 \text{ GeV}$$

$$M_Z = \frac{M_W}{\cos^2\theta_W} = 88.7 \text{ GeV}$$

$$\Gamma_W = \frac{\alpha M_W}{24 \sin^2\theta_W}\left(3n_q + n_\ell\right) = 2.47 \text{ GeV} \qquad (6)$$

$$\Gamma_{Z^0} = \frac{1}{3}\frac{\alpha M_Z}{\sin^2\theta_W \cos^2\theta_W}\left\{3\sum_q\left[\left(a^q\right)^2 + \left(b^q\right)^2\right] + \sum_\ell\left[\left(a^\ell\right)^2 + \left(b^\ell\right)^2\right] = 2.49 \text{ GeV}\right.$$

In the above, n_q is the number of quark flavours and n_ℓ is the number of leptons, for which we take the value $n_\ell = n_q = 6$.

3. SINGLE LEPTONS FROM POLARIZED PROTONS

In this section we calculate polarization effects for single leptons from the decays of $W^\pm$ in $\bar{p}p$ collisions with polarized protons. This process is described by the diagram of Fig. 1b, where P_1 and P_2 are the momenta of the beam and target hadrons, p_1 and p_2 are those of the partons from beam and target hadron, respectively, and k is the momentum of the observed lepton. The unobserved neutrino momentum P_X is given by

$$P_X = P_1 + P_2 - k \ . \qquad (7)$$

We fix the positive z axis in the direction of the antiproton. Because of the axial symmetry of the process we can choose a frame where the lepton momentum lies in the xz plane in the c.m.s. of the incident particles, namely

$$k = (k_0, k_T, 0, k_L) \ . \qquad (8)$$

The polar angle θ is defined by the equations

$$k_T = k_0 \sin\theta$$
$$k_L = k_0 \cos\theta \qquad (9)$$

and the rapidity of the lepton by

$$k_0 = k_T \cosh y$$
$$k_L = k_T \sinh y \ . \tag{10}$$

These variables are related as

$$e^{-y} = \tan \theta/2 \ . \tag{11}$$

The kinematical boundary condition reads

$$p_X^2 \geq 0 \quad \text{or} \quad k_0 < \frac{\sqrt{s}}{2} \ . \tag{12}$$

We use the result of Eq. (2) in Section 2 to calculate the parton level cross-sections, which in the inclusive case are given by

$$k_0 \frac{d\hat{\sigma}^{j,k}}{d^3k} = \frac{1}{2} \frac{1}{2\hat{s}} \frac{1}{(2\pi)^2} \delta(\hat{s} + \hat{t} + \hat{u}) \overline{|m_{j,k}|^2} \ , \tag{13}$$

where j and k are the appropriate partons in the process, $\hat{s} = 2p_1 \cdot p_2$, $\hat{t} = -2p_1 \cdot k$, and $\hat{u} = -2p_2 \cdot k$. The cross-section at the hadron level is obtained from this by integrating over the parton distributions

$$k_0 \frac{d\sigma}{d^3k} = \sum_{j,k} \int_0^1 d\xi_1 \ f^j(\xi_1, k_T^2) \int_0^1 d\xi_2 \ f^k(\xi_2, k_T^2) \ k_0 \frac{d\hat{\sigma}^{j,k}}{d^3k} \ . \tag{14}$$

In the above ξ_1 and ξ_2 are the longitudinal momentum fractions and $f^j(\xi_i, k_T^2)$ is the non-scaling parton-distribution function of parton j in hadron i. We have chosen the large scale $Q^2 = k_T^2$ as the scale parameter for the quark distributions. The integration path in the (ξ_1, ξ_2) plane is determined by the δ function

$$\delta(\hat{s} + \hat{t} + \hat{u}) = \frac{1}{s} \delta\left(\xi_1\xi_2 - \frac{k_T}{\sqrt{s}} e^{-y} \xi_1 - \frac{k_T}{\sqrt{s}} e^{y} \xi_2\right) ,$$

which is a hyperbola. The integration path can be simplified by introducing the variables (x_1, x_2) defined as

$$\xi_i = \frac{X_i}{x_i} \qquad (i = 1,2) \tag{15}$$

with

$$X_1 = \frac{k_T^2}{2P_1 \cdot k} = \frac{k_T}{\sqrt{s}} e^{y}$$
$$X_2 = \frac{k_T^2}{2P_2 \cdot k} = \frac{k_T}{\sqrt{s}} e^{-y} \; . \tag{16}$$

Then Eq. (14) takes the form

$$k_0 \frac{d\sigma}{d^3k} = \sum_{j,k} \int_{X_1}^{1-X_2} \frac{dx_1}{x_1} \left[\xi_1 f^j(\xi_1)\right] \int_{X_2}^{1-x_1} \frac{dx_2}{x_2} \left[\xi_2 f^k(\xi_2)\right] k_0 \frac{d\hat{\sigma}^{j,k}}{d^3k} \; . \tag{17}$$

The invariants can now be expressed as

$$\hat{s} = \frac{k_T^2}{x_1 x_2} \; , \quad \hat{t} = -\frac{k_T^2}{x_1} \; , \quad \hat{u} = -\frac{k_T^2}{x_2} \; ,$$

and similarly the δ function

$$\delta(\hat{s} + \hat{t} + \hat{u}) = \frac{1}{\hat{s}} \delta(1 - x_1 - x_2) \; .$$

It remains now to calculate explicitly the elementary cross-sections for polarized partons. We denote the quark helicity by h_q and the antiquark helicity by $h_{\bar{q}}$. In the case of $W^{\pm}$ the cross-sections for polarized partons are obtained from those for unpolarized ones by multiplying with the factor

$$H = \left(1 - h_q h_{\bar{q}}\right)\left(1 - h_q\right)$$
$$= \left(1 - h_q h_{\bar{q}}\right)\left(1 + h_{\bar{q}}\right) \; . \tag{18}$$

H vanishes for $h_q = +1$ or $h_{\bar{q}} = -1$, which tells us that in V-A theory $W^{\pm}$ couples only to left-handed quarks and right-handed antiquarks. For unpolarized quarks there are the following possibilities:

$$
\begin{aligned}
k_0 \frac{d\hat{\sigma}}{d^3k}\,(u + \bar{d} \to W^+ \to \bar{\ell} + X) &= N(\hat{s})\ \hat{t}^2 \\
k_0 \frac{d\hat{\sigma}}{d^3k}\,(d + \bar{u} \to W^- \to \ell + X) &= N(\hat{s})\ \hat{u}^2 \\
k_0 \frac{d\hat{\sigma}}{d^3k}\,(\bar{d} + u \to W^+ \to \bar{\ell} + X) &= N(\hat{s})\ \hat{u}^2 \\
k_0 \frac{d\hat{\sigma}}{d^3k}\,(\bar{u} + d \to W^- \to \ell + X) &= N(\hat{s})\ \hat{t}^2\ ,
\end{aligned}
\tag{19}
$$

with

$$
N(\hat{s}) = \frac{1}{3}\,\frac{\alpha^2}{4\,\sin^4\theta_W}\,\frac{1}{\left(\hat{s} - M_W^2\right)^2 + \left(\Gamma_W M_W\right)^2}\,\frac{1}{\hat{s}}\,\delta(\hat{s} + \hat{t} + \hat{u})\ . \tag{20}
$$

The cross-sections for polarized partons follow from these by applying Eq. (18). Then for W^+

$$
\begin{aligned}
k_0 \frac{d\hat{\sigma}}{d^3k}\,(u_- \bar{d}_+ \to W^+ \to \bar{\ell}X) &= 4\ N(\hat{s})\ \hat{t}^2 \\
k_0 \frac{d\hat{\sigma}}{d^3k}\,(u_+ \bar{d}_- \to W^+ \to \bar{\ell}X) &= 0 \\
k_0 \frac{d\hat{\sigma}}{d^3k}\,(u_- \bar{d}_- \to W^+ \to \bar{\ell}X) &= 0 \\
k_0 \frac{d\hat{\sigma}}{d^3k}\,(u_+ \bar{d}_+ \to W^+ \to \bar{\ell}X) &= 0\ .
\end{aligned}
\tag{21}
$$

In the above we have used the notation where, for instance, u_- denotes a u quark with helicity $h_q = -1$ and $\bar{d}_+$ a $\bar{d}$ quark with $h_{\bar{q}} = +1$. One should also remember that following our conventions the first parton always comes from the beam hadron with momentum p_1 and the second from the target hadron with momentum p_2.

The sea quarks are assumed to be unpolarized. Therefore we need the cross-sections in the case where only one of the partons is polarized:

$$
\begin{aligned}
k_0 \frac{d\hat{\sigma}}{d^3k} (u\bar{d}_+ \to W^+ \to \bar{\ell}X) &= 2\, N(\hat{s})\, \hat{t}^2 \\
k_0 \frac{d\hat{\sigma}}{d^3k} (u_-\bar{d} \to W^+ \to \bar{\ell}X) &= 2\, N(\hat{s})\, \hat{t}^2 \\
k_0 \frac{d\hat{\sigma}}{d^3k} (u_+\bar{d} \to W^+ \to \bar{\ell}X) &= 0 \\
k_0 \frac{d\hat{\sigma}}{d^3k} (u\bar{d}_- \to W^+ \to \bar{\ell}X) &= 0 \ ,
\end{aligned}
\tag{22}
$$

which follow directly from Eqs. (21).

To calculate the cross-section at the hadron level we need the distributions for polarized partons. In the proton with definite helicity a quark can be either in the state $h_q = +1$ or $h_q = -1$. The relation between the proton helicity and quark helicity is provided, for instance, by the SU(6) model[7], which predicts

$$
\begin{aligned}
u^v_{++} = u^v_{--} &= \frac{5}{6} u^v \qquad & d^v_{++} = d^v_{--} &= \frac{1}{3} d^v \\
u^v_{+-} = u^v_{-+} &= \frac{1}{6} u^v \qquad & d^v_{+-} = d^v_{-+} &= \frac{2}{3} d^v \ .
\end{aligned}
\tag{23}
$$

In the above the first subscript refers to the quark helicity and the second to the helicity of the proton. Then, for instance, u_{+-} is the distribution of a right-handed u quark in a left-handed proton. For convenience we use in the following formulae the abbreviation $\sigma = \sum_{j,k} f^j f^k \hat{\sigma}^{jk}$ for the cross-section

$$
k_0 \frac{d\sigma}{d^3k} = \sum_{j,k} \int_0^1 d\xi_1\, f^j(\xi_1, k_T^2) \int_0^1 d\xi_2\, f^k(\xi_2, k_T^2)\, k_0 \frac{d\hat{\sigma}^{jk}}{d^3k} \ .
$$

Furthermore we denote by f_+ (f_-) the distribution of the quark with the same (opposite) helicity as its parent hadron. Note here the difference from Eqs. (21) and (22), where the subscripts of the parton distributions refer only to the quark helicity. For the parton distribution function f, we use the general decomposition to valence and sea parts, $f^u = u^v + s$ and $f^d = d^v + s$, assuming the sea quark component to be SU(3)-symmetric. Summing up the different contributions, we get

$$\begin{aligned}
\sigma(\bar{p}_+p_+) &= 2\hat{u}^2\ d_+^V s + 2\hat{u}^2\ s u_-^V + 4\hat{u}^2\ d_+^V u_-^V + (\hat{t}^2 + \hat{u}^2)ss \\
\sigma(\bar{p}_-p_+) &= 2\hat{u}^2\ d_-^V s + 2\hat{u}^2\ s u_-^V + 4\hat{u}^2\ d_-^V u_-^V + (\hat{t}^2 + \hat{u}^2)ss \\
\sigma(\bar{p}_-p_-) &= 2\hat{u}^2\ d_-^V s + 2\hat{u}^2\ s u_+^V + 4\hat{u}^2\ d_-^V u_+^V + (\hat{t}^2 + \hat{u}^2)ss \\
\sigma(\bar{p}_+p_-) &= 2\hat{u}^2\ d_+^V s + 2\hat{u}^2\ s u_+^V + 4\hat{u}^2\ d_+^V u_+^V + (\hat{t}^2 + \hat{u}^2)ss\ ,
\end{aligned} \tag{24}$$

where we have again simplified the notation by omitting the factor $N(\hat{s})$ on the right-hand side and $W^+ \to \bar{\ell}X$ in the arguments of σ and denoting the hadron helicity by a subscript (+ or −).

The cross-sections when only the proton is polarized follow from Eqs. (24) by averaging over the antiproton helicities

$$\begin{aligned}
\sigma(\bar{p}p_+) &= \hat{u}^2\ d^V s + 2\hat{u}^2\ s u_-^V + 2\hat{u}^2\ d^V u_-^V + (\hat{t}^2 + \hat{u}^2)ss \\
\sigma(\bar{p}p_-) &= \hat{u}^2\ d^V s + 2\hat{u}^2\ s u_+^V + 2\hat{u}^2\ d^V u_+^V + (\hat{t}^2 + \hat{u}^2)ss\ .
\end{aligned} \tag{25}$$

Using the SU(6) predictions shown in Eqs. (24), we finally get

$$\begin{aligned}
\sigma(\bar{p}p_+) &= (d^V + s)\left(\frac{1}{3}\,u^V + s\right)\hat{u}^2 + ss\ \hat{t}^2 \\
\sigma(\bar{p}p_-) &= (d^V + s)\left(\frac{5}{3}\,u^V + s\right)\hat{u}^2 + ss\ \hat{t}^2\ .
\end{aligned} \tag{26}$$

The cross-sections for W^- by polarized protons are obtained from Eq. (26) by the change $\hat{t} \leftrightarrow \hat{u}$ and $u^V \leftrightarrow d^V$. We define the asymmetry parameter as

$$A_{LL} = \frac{\sigma(\bar{p}p_-) - \sigma(\bar{p}p_+)}{\sigma(\bar{p}p_-) + \sigma(\bar{p}p_+)} = \frac{2}{3}\,\frac{\int_0^1 N(\hat{s})\,\left[(d^V + s)u^V\right]\hat{u}^2\,d\xi_1\,d\xi_2}{\int_0^1 N(\hat{s})\,\left[d^V + s)(u^V + s)\hat{u}^2 + ss\ \hat{t}^2\right]\,d\xi_1\,d\xi_2} \tag{27}$$

which obtains the value $^2/_3$ if sea interactions are negligible. Furthermore, it can be seen that the asymmetry vanishes when the c.m.s. energy goes to infinity.

In the above we calculated the differential cross-section $k_0\, d\sigma/d^3k$, but it is more useful to present the distributions in k_T and cos θ. The change of variables is performed by multiplying with the Jacobian $k_T/\sin^2\theta$:

$$\frac{d\sigma}{dk_T d\Omega} = \frac{k_T}{\sin^2\theta}\, k_0\, \frac{d\sigma}{d^3k} \,. \tag{28}$$

The polarization effects for single leptons from the Fermi theory of weak interactions without W are obtained from Eqs. (26) with $M_W = \infty$ and $\Gamma_W = 0$.

4. LEPTON PAIRS FROM Z^0 and γ

Next we calculate the polarization effects for the production of lepton pairs from Z^0 and γ. The process is shown in Fig. 1c, where k_1 and k_2 are the momenta of the observed leptons and for other variables the notation is the same as in Fig. 1b. We use the axial symmetry of the process when choosing the variables. Then in the c.m.s. of the lepton pair

$$\begin{aligned} k_1 &= \frac{M}{2}\,(1,\ \sin\theta,\ 0,\ \cos\theta) \\ k_2 &= \frac{M}{2}\,(1,\ -\sin\theta,\ 0,\ -\cos\theta) \\ p_1 &= \frac{M}{2}\,(1,\ 0,\ 0,\ 1) \\ p_2 &= \frac{M}{2}\,(1,\ 0,\ 0,\ -1)\ , \end{aligned} \tag{29}$$

where $M^2 = (k_1 + k_2)^2$ is the invariant mass of the lepton pair. The invariants can now be written in the form

$$\begin{aligned} \hat{s} &= M^2 \\ \hat{t} &= -2p_1k_1 = -\frac{M^2}{2}\,(1 - \cos\theta) \\ \hat{u} &= -2p_2k_1 = -\frac{M^2}{2}\,(1 + \cos\theta)\ . \end{aligned} \tag{30}$$

The cross-section for the quark process follows from Eq. (2). Because Z^0 interferes with γ the amplitude is the sum of Z^0 and γ contributions. The cleanest signal of Z^0 should be obtained in the invariant mass spectrum of the lepton pairs.

Therefore we write down the cross-section $d\sigma/dM^2 d\Omega$, where Ω is the solid angle of one of the leptons in the rest system of the lepton pair. At the parton level this cross-section is given by

$$\frac{16\pi}{3}\frac{d\hat{\sigma}}{dM^2 d\Omega} = \left(1 - h_q h_{\bar{q}}\right)\left\langle\frac{1}{3}\right\rangle \delta(\hat{s} - M^2)\,\frac{4\pi\alpha^2}{3M^2}\left\{Q_q^2\,(1 + \cos^2\theta)\right.$$

$$+ \frac{A^q + h_q B^q}{\sin^4\theta_W \cos^4\theta_W}\,\frac{M^4}{\left(M^2 - M_Z^2\right)^2 + \left(\Gamma_Z M_Z\right)^2}\left[A^\ell(1 + \cos^2\theta) + 2h_q B^\ell \cos\theta\right]$$

$$\left. - 2Q_q\,\frac{a^q + h_q b^q}{\sin^2\theta_W \cos^2\theta_W}\,\frac{M^2\left(M^2 - M_Z^2\right)}{\left(M^2 - M_Z^2\right)^2 + \left(\Gamma_Z M_Z\right)^2}\left[a^\ell(1 + \cos^2\theta) + 2h_q b^\ell \cos\theta\right]\right\}. \tag{31}$$

The last term is the interference contribution between γ and Z^0. With the present value of the Weinberg angle θ_W this term is small and we shall neglect it in the following. The $1 + \cos^2\theta$ behaviour of the angular distribution arises from the vector part of the coupling and the $\cos\theta$ behaviour from the parity-violating axial part.

To obtain the physical cross-sections for polarized hadrons, we have to convolute the above result with the distribution functions for polarized partons. To this end we first define the functions $\Theta_u(h_q, h_{\bar{q}})$ and $\Theta_d(h_q, h_{\bar{q}})$ using the numerical values of $\sin^2\theta_W$ and Q_q:

$$\Theta_u(h_q, h_{\bar{q}}) = \left(1 - h_q h_{\bar{q}}\right)\left\{\frac{4}{9}(1 + \cos^2\theta)\right.$$
$$\left. + (0.145 - 0.097\,h_q)(1 + \cos^2\theta - 0.32\,h_q\cos\theta)\,M^4\,BW\right\}$$

$$\Theta_d(h_q, h_{\bar{q}}) = \left(1 - h_q h_{\bar{q}}\right)\left\{\frac{1}{9}(1 + \cos^2\theta)\right. \tag{32}$$
$$\left. + (0.186 - 0.175\,h_q)(1 + \cos^2\theta - 0.32\,h_q\cos\theta)\,M^4\,BW\right\}$$

where

$$BW = \frac{1}{\left(M^2 - M_Z^2\right)^2 + \left(\Gamma_Z M_Z\right)^2}\,.$$

The sea quarks are not polarized. For the case when the antiquark is unpolarized we need the above functions averaged over antiquark helicities:

$$\Theta_u(h_q) = \frac{4}{9}(1 + \cos^2\theta) + (0.145 - 0.097\, h_q)(1 + \cos^2\theta - 0.32\, h_q \cos\theta)\, M^4\, BW$$

$$\Theta_d(h_q) = \frac{1}{9}(1 + \cos^2\theta) + (0.186 - 0.175\, h_q)(1 + \cos^2\theta - 0.32\, h_q \cos\theta)\, M^4\, BW \tag{33}$$

and when the quark is unpolarized

$$\bar{\Theta}_u(h_{\bar{q}}) = \frac{4}{9}(1 + \cos^2\theta) + (0.145 + 0.097\, h_{\bar{q}})(1 + \cos^2\theta + 0.32\, h_{\bar{q}} \cos\theta)\, M^4\, BW$$

$$\bar{\Theta}_d(h_{\bar{q}}) = \frac{1}{9}(1 + \cos^2\theta) + (0.186 + 0.175\, h_{\bar{q}})(1 + \cos^2\theta + 0.32\, h_{\bar{q}} \cos\theta)\, M^4\, BW \tag{34}$$

and finally when both of the quarks are unpolarized

$$\Theta_u = \frac{4}{9}(1 + \cos^2\theta) + 0.145\,(1 + \cos^2\theta + 0.214\cos\theta)\, M^4\, BW$$

$$\Theta_d = \frac{1}{9}(1 + \cos^2\theta) + 0.186\,(1 + \cos^2\theta + 0.301\cos\theta)\, M^4\, BW\,. \tag{35}$$

It should be noted that the parton cross-section in Eq. (31) is written for the case where the quark is in the beam hadron (antiquark in the target) and the angular distribution is that of the lepton. In our conventions the antiproton is the beam hadron. Therefore to include the valence-valence interactions we exchange the roles of q and $\bar{q}$ in our formulae and consequently the obtained angular distribution is for the antilepton. Because the axial part for the sea-sea interaction is of opposite sign to that for the valence-valence interaction we make the change $\cos\theta \to -\cos\theta$ in the Θ functions defined by Eqs. (32)-(35).

We are now ready to write down the cross-section when both proton and antiproton are polarized with helicities h and $\bar{h}$ (+ or −):

$$\frac{16\pi}{3}\frac{d\sigma}{dM^2 d\Omega}(\bar{h},h) = \frac{4\pi\alpha^2}{3M^2}\left\langle\frac{1}{3}\right\rangle\int d\xi_1\, d\xi_2\, \delta(\hat{s}-M^2)$$

$$\times\Big\{u_{\bar{h}-}^{v}u_{h+}^{v}\Theta_u(+,-) + u_{\bar{h}+}^{v}u_{h-}^{v}\Theta_u(-,+)$$

$$+ u_{\bar{h}+}^{v}s\bar{\Theta}_u(+) + u_{\bar{h}-}^{v}s\bar{\Theta}_u(-)$$

$$+ su_{h-}^{v}\Theta_u(-) + su_{h+}^{v}\Theta_u(+)$$

$$+ ss\left[\Theta_u + \Theta_u\ (\cos\theta \to -\cos\theta)\right] + (u \leftrightarrow d)\Big\}\,. \qquad (36)$$

The cross-section for antiprotons and polarized protons is obtained from Eq. (35) by averaging over the antiproton helicities. Introducing also the SU(6) parton distributions we get

$$\frac{d\sigma}{dM^2 d\Omega}(\bar{p}p_+) = \frac{3}{16\pi}\frac{4\pi\alpha^2}{3M^2}\left\langle\frac{1}{3}\right\rangle\int d\xi_1\, d\xi_2\, \delta(\hat{s}-M^2)$$

$$\times\Big\{(u_v+s)u_v\cdot\frac{1}{6}\left[5\,\Theta_u(+)+\Theta_u(-)\right]$$

$$+ (u_v+s)s\cdot\Theta_u + ss\cdot\Theta_u\ (\cos\theta\to-\cos\theta)$$

$$+ (d_v+s)d_v\cdot\frac{1}{3}\left[\Theta_d(+)+2\,\Theta_d(-)\right]$$

$$+ (d_v+s)s\cdot\Theta_d + ss\cdot\Theta_d\ (\cos\theta\to-\cos\theta)\Big\}\,. \qquad (37)$$

$$\frac{d\sigma}{dM^2 d\Omega}(\bar{p}p_-) = \frac{3}{16\pi}\frac{4\pi\alpha^2}{3M^2}\left\langle\frac{1}{3}\right\rangle\int d\xi_1\, d\xi_2\, \delta(\hat{s}-M^2)$$

$$\times\Big\{(u_v+s)u_v\cdot\frac{1}{6}\left[\Theta_u(+)+5\,\Theta_u(-)\right]$$

$$+ (u_v+s)s\cdot\Theta_u + ss\cdot\Theta_u\ (\cos\theta\to-\cos\theta)$$

$$+ (d_v+s)d_v\cdot\frac{1}{3}\left[\Theta_d(+)+\Theta_d(-)\right]$$

$$+ (d_v+s)s\cdot\Theta_d + ss\cdot\Theta_d\ (\cos\theta\to-\cos\theta)\Big\}\,. \qquad (38)$$

We can further simplify the above formulae by defining still another function Δ_f (f = u,d) by

$$\Theta_f(h_q) = \Theta_f - h_q \Delta_f \ , \tag{39}$$

where

$$\begin{aligned} \Delta_u &= \left[0.097\ (1 + \cos^2\theta) + 0.046 \cos\theta\right] M^4\ BW \\ \Delta_d &= \left[0.175\ (1 + \cos^2\theta) + 0.060 \cos\theta\right] M^4\ BW \end{aligned} \tag{40}$$

Then we can write the final result in a simple form

$$\begin{aligned} \frac{d\sigma}{dM^2 d\Omega_{\ell^+}} (\bar{p}p_{\pm} \to \gamma + Z^0 \to \ell^+\ell^-) = \frac{3}{16\pi} \left\langle \frac{1}{3} \right\rangle \frac{4\pi\alpha^2}{3M^2} \int d\xi_1\ d\xi_2\ \delta(\hat{s} - M^2) \\ \times \Big\{ (s + u_v)\, u_v \left[\Theta_u \mp \frac{2}{3} \Delta_u\right] + (u_v + s) s \cdot \Theta_u \\ + ss \cdot \Theta_u\ (\cos\theta \to -\cos\theta) \\ + (s + d_v)\, d_v \left[\Theta_d \pm \frac{1}{3} \Delta_d\right] + (d_v + s) s \cdot \Theta_d \\ + ss \cdot \Theta_d\ (\cos\theta \to -\cos\theta) \Big\} \ . \end{aligned} \tag{41}$$

The angular distribution for the antilepton is obtained from this by the change $\cos\theta \to -\cos\theta$.

5. HIGHER ORDER QCD CORRECTIONS?

The leading logarithmic QCD correction is included in our calculations by using non-scaling distribution functions. Higher order QCD corrections have been studied by Aurenche and Lindfors[6]. For the lepton-pair spectrum from Z^0 the $\Theta(\alpha_s)$ QCD corrections normalize the Drell-Yan result upwards by about 30-40%. Polarization asymmetry will not be affected essentially by these QCD corrections, because the main correction terms are similar for the vector and axial parts.

The transverse momentum spectrum of the observed lepton from $W^{\pm}$ changes significantly by the higher order QCD corrections. At $k_T < M_W/2$ the spectrum is normalized by about 50-100%, the peak at $M_W/2$ is somewhat smeared, and above the

peak the QCD terms dominate clearly. The angular distribution is normalized but the shape remains essentially the same. Again the QCD corrections are similar for vector and axial parts and hence the corrections for polarization asymmetries will not be as significant as for the k_T spectrum.

6. NUMERICAL CALCULATIONS

We calculate the numerical examples for the CERN $\bar{p}p$ collider and the Fermilab Tevatron, i.e. at the c.m.s. energies of $\sqrt{s}$ = 540 GeV and 2000 GeV. We use the parametrizations of Owens and Reya[8] for the non-scaling parton distribution functions.

First we present the results for single leptons from W^+. In Fig. 2a we show the differential cross-section $d\sigma/dk_T d\Omega$ for the antilepton (e^+ or μ^+) at $\sqrt{s}$ = = 540 GeV as a function of k_T for different values of cos θ and in Fig. 2b the same cross-section as a function of cos θ for different values of k_T. The cross-section corresponding to the positive and negative helicity of the proton are shown separately as dashed and solid curves.

At low k_T values the cross-section is strongly peaked in the forward direction. This is a consequence of helicity conservation, which forces the antilepton to move in the direction of the antiproton. The peak is further enhanced by the Jacobian $k_T/\sin^2\theta$ near cos θ = 1. However, when the transverse momentum of the lepton reaches the value $M_W/2$ the lepton can no longer have longitudinal momentum in the rest frame of W. Hence the longitudinal motion of the lepton in the c.m.s. of the incident hadrons reflects that of the parent particle. The turnover of the angular distribution at high k_T values follows from the used parametrizations of parton distributions[8] where a u quark in the proton is provided with larger average momentum than the d quark.

The distribution corresponding to the negative helicity of the proton is seen to be more than 2-5 times larger than the distribution from the proton with positive helicity. The variation of the polarization asymmetry [defined in Eq. (27)] as a function of k_T and cos θ, is better demonstrated in Fig. 3, which shows the

asymmetry as a function of cos θ for different k_T values and the asymmetry integrated over the k_T range 25-50 GeV/c. At low k_T values the asymmetry is small in the backward (proton) direction. This is explained by the angular behaviour of the different terms in the asymmetry formula [$\hat{t} \approx \tan \theta/2$, $\hat{u} \approx \cot \theta/2$]. The integrated asymmetry (with the k_T cut), which probably is the most interesting quantity, is large ($\sim$ 0.6) and essentially constant except near cos θ = 1, where it is somewhat smaller.

Figure 4 shows the asymmetry as a function of k_T and integrated over the angles at the c.m.s. energies of $\sqrt{s}$ = 540 GeV and $\sqrt{s}$ = 2000 GeV. Again the asymmetry is nearly constant over the whole k_T range. However it tends to increase at $k_T > M_W/2$, approaching the value of $^2/_3$ because the sea-quark interactions become negligible at high transverse momenta.

In Figs. 5a and 5b we show the k_T and cos θ distributions and in Fig. 6 the asymmetry at the Tevatron energies. The shapes of the angular distributions are changed considerably, being now peripheral over the whole k_T range. The polarization asymmetry is somewhat smaller here, whereas the forward-backward asymmetry at $k_T = M_W/2$ is substantially larger. The integrated polarization asymmetry as a function of cos θ is at a maximum ($\sim$ 0.6) in the backward direction and decreases in the forward direction ($\sim$ 0.2).

The polarization effects for single-lepton production in weak interactions without W are shown in Figs. 7a and 7b at collider energies. Figure 7a presents the k_T distribution of the positive lepton for infinitely heavy W at cos θ = 0 and Fig. 7b the angular distribution at k_T = 200 GeV/c. The cross-section decreases by about two orders of magnitude from the peak value of the W cross-section, but is relatively large still at very high k_T values. The polarization asymmetry obtains its maximum value $A_{LL} = {}^2/_3$ in the central region at high transverse momenta. In the case where W does not exist this asymmetry effect would be important to separate the leptons coming from electromagnetic and weak interactions.

Figures 8-12 give the predictions for polarization effects in lepton-pair production from Z^0. We have used here the same definition for the asymmetry parameter as in Eq. (27) for $W^{\pm}$. The differential cross-section $d\sigma/dM^2d\Omega$ at collider energies is presented in Fig. 8 as a function of M at $\cos\theta = 0$, where θ is the polar angle of the antilepton (μ^+ or e^+) in the rest frame of Z^0, and in Fig. 9 as a function of $\cos\theta$ at $M = M_Z$. The same distributions for the Tevatron energies are shown in Figs. 10 and 11. The polarization asymmetries, being non-zero only at the Z^0 peak, are presented in Fig. 12 as a function of $\cos\theta$ at $M = M_Z$. They increase slightly in the forward direction, being 0.2-0.5 at collider energies and very small, 0.05-0.1, at Tevatron energies. We note that here the polarization asymmetry, although fairly small, might be valuable because the forward-backward asymmetry in the Z^0 peak is not large.

7. CONCLUSIONS

We have studied the polarization effects for lepton production from $W^{\pm}$ and Z^0 decays in $\bar{p}p$ collisions with a longitudinally polarized proton beam. The cross-sections have been calculated from the Drell-Yan process, using the standard $SU(2) \times U(1)$ model. The leading logarithmic QCD effect is also included in our calculation. To obtain the physical cross-sections at the hadron level we have used the predictions of the SU(6) model for the parton distributions in the longitudinally polarized proton.

Large polarization effects were found for the $\bar{p}p$ storage rings now under construction. At the CERN $\bar{p}p$ collider the asymmetry parameter A_{LL} for single leptons from $W^{\pm}$ is $A_{LL} \approx 0.6$ and for lepton pairs from Z^0 $A_{LL} \approx 0.2$. At the energies of the Fermilab Tevatron the polarization asymmetry was found to be already somewhat smaller, $A_{LL} \approx 0.4$ in the case of single leptons from $W^{\pm}$ and $A_{LL} \lesssim 0.1$ for lepton pairs from Z^0. For the production of single leptons from point-like interactions without weak bosons the asymmetry would be large, $A_{LL} \approx 2/3$, at high transverse momenta of the produced lepton. The asymmetries do not vary significantly as a function of one kinematic variable.

Our conclusion is that the polarization effects will give valuable information in the study of weak bosons in $\bar{p}p$ collisions at high energies.

Acknowledgements

We would like to thank C. Rubbia for many discussions and for pointing out to us the importance of studying the polarization effects for weak boson production. We wish also to thank P. Aurenche for discussions.

REFERENCES

1) E.D. Courant and R.D. Ruth, Depolarization of polarized protons in circular accelerators, BNL 51270 (1970), and references therein.

2) H.E. Haber and G.L. Kane, Nucl. Phys. B146, 109 (1978).

3) F.E. Paige, T.L. Trueman and T.N. Tudron, Phys. Rev. D 19, 935 (1979).

4) F.E. Paige, Talk at Topical Conference on the Production of New Particles in Super High Energy Collisions, Madison, October 1979.

5) R.F. Peierls, T.L. Trueman and Ling-Lie Wang, Phys. Rev. D 16, 1397 (1977).
C. Quigg, Rev. Mod. Phys. 94, 297 (1977).
L.B. Okun and M.B. Voloshin, Nucl. Phys. B120, 459 (1977).

6) P. Aurenche and J. Lindfors, Phys. Lett. 96B, 171 (1980).

7) L.M. Sehgal, Phys. Rev. D 10, 1663 (1974).
F.E. Close, Nucl. Phys. B80, 269 (1974).

8) J.F. Owens and E. Reya, Phys. Rev. D 17, 3003 (1978).

Figure captions

Fig. 1 : a) The Feynman diagram for the Drell-Yan process $q\bar{q} \to \ell\bar{\ell}$.

b) The schematic diagram for single-lepton production in hadron collisions.

c) The schematic diagram for lepton-pair production in hadron collisions.

Fig. 2 : Single-lepton cross-sections for positive (dashed curve) and negative (solid curve) helicity of the proton in the reaction $\bar{p}p \to W^+ \to \ell^+X$ at $\sqrt{s}$ = 540 GeV

a) as a function of p_T for different values of cos θ;

b) as a function of cos θ for different values of p_T.

Fig. 3 : The polarization asymmetry for the reaction $\bar{p}p \to W^+ \to \ell^+X$ at $\sqrt{s}$ = 540 GeV as a function of cos θ for p_T = 10 GeV/c (dashed curve), p_T = 30 GeV/c (dash-dotted curve), p_T = 38.9 GeV/c (dotted curve) and the asymmetry integrated over the p_T range 25-50 GeV/c (solid curve).

Fig. 4 : The polarization asymmetry for the reaction $\bar{p}p \to W^+ \to \ell^+X$ at $\sqrt{s}$ = 540 GeV and $\sqrt{s}$ = 2000 GeV as a function of p_T and integrated over the angles.

Fig. 5 : Single-lepton cross-sections for positive (dashed curve) and negative (solid curve) helicity of the proton in the reaction $\bar{p}p \to W^+ \to \ell^+X$ at $\sqrt{s}$ = 2000 GeV

a) as a function of p_T for different values of cos θ;

b) as a function of cos θ for different values of p_T.

Fig. 6 : The polarization asymmetry for the reaction $\bar{p}p \to W^+ \to \ell^+X$ at $\sqrt{s}$ = 2000 GeV as a function of cos θ for p_T = 10 GeV/c (dashed curve), p_T = 30 GeV/c (dash-dotted curve), p_T = 38.9 GeV/c (dotted curve) and the asymmetry integrated over the p_T range 25-50 GeV/c (solid curve).

Fig. 7 : Single-lepton cross-sections in the weak interactions without W ($M_W = \infty$) for the reaction $\bar{p}p \to \ell^+ X$ at $\sqrt{s}$ = 540 GeV
a) as a function of p_T at $\cos\theta = 0$,
b) as a function of $\cos\theta$ at p_T = 200 GeV/c.
The curves correspond to the positive ($h_p = +1$) and negative ($h_p = -1$) helicity proton.

Fig. 8 : The differential cross-section $d\sigma/dM^2d\Omega$ for lepton pairs in the reaction $\bar{p}p \to \gamma + Z^0 \to \ell^+\ell^- + X$ at $\sqrt{s}$ = 540 GeV as a function of M at $\cos\theta = 0$.

Fig. 9 : The angular distributions for ℓ^+ in the reaction $\bar{p}p \to \gamma + Z^0 \to \ell^+\ell^- + X$ at $\sqrt{s}$ = 540 GeV in the rest frame of Z^0 at $M = M_Z$. The solid curve corresponds to the negative and the dashed curve to the positive helicity of the proton.

Fig. 10 : The differential cross-section $d\sigma/dM^2d\Omega$ for lepton pairs in the reaction $\bar{p}p \to \gamma + Z^0 \to \ell^+\ell^- + X$ at $\sqrt{s}$ = 2000 GeV as a function of M at $\cos\theta = 0$.

Fig. 11 : The angular distributions for ℓ^+ in the reaction $\bar{p}p \to \gamma + Z^0 \to \ell^+\ell^- + X$ at $\sqrt{s}$ = 2000 GeV in the rest frame of Z^0 at $M = M_Z$. The solid curve corresponds to the negative and the dashed curve to the positive helicity of the proton.

Fig. 12 : The polarization asymmetry for the reaction $\bar{p}p \to \gamma + Z^0 \to \ell^+\ell^- + X$ at the c.m.s. energies of $\sqrt{s}$ = 540 GeV and $\sqrt{s}$ = 2000 GeV as a function of $\cos\theta$ at $M = M_Z$.

a)

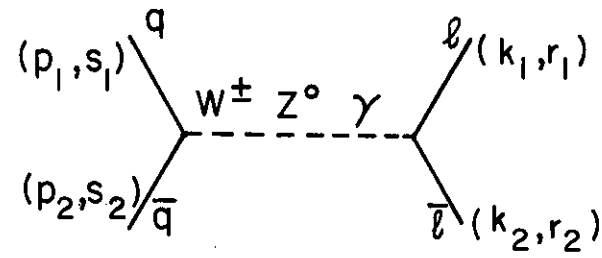
q
(p_1, s_1)
$W^{\pm}$ Z° γ
ℓ (k_1, r_1)
(p_2, s_2) $\bar{q}$
$\bar{\ell}$ (k_2, r_2)

b)

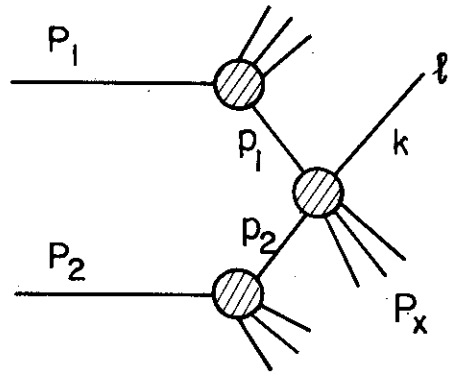
P_1
ℓ
p_1
k
p_2
P_2
P_x

c)

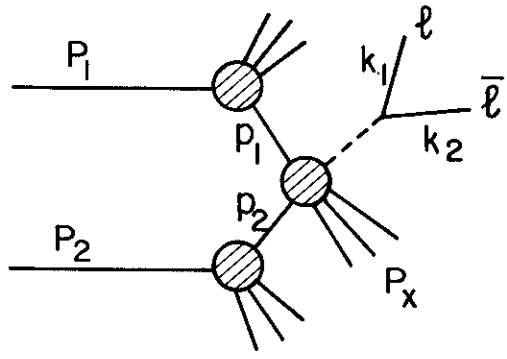
P_1
k_1
ℓ
$\bar{\ell}$
p_1
k_2
p_2
P_2
P_x

Fig. 1

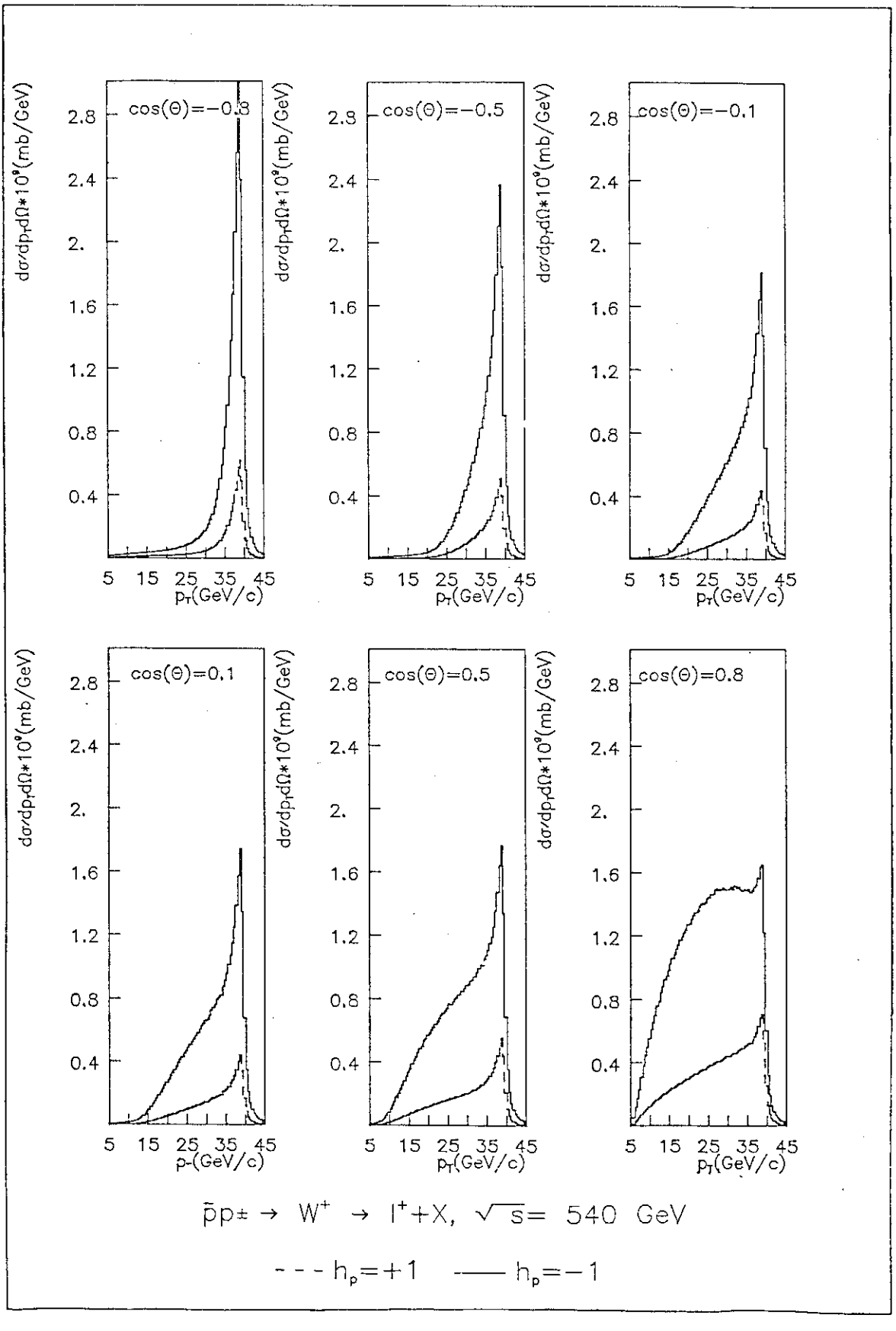
cos(Θ)=−0.8
cos(Θ)=−0.5
cos(Θ)=−0.1
cos(Θ)=0.1
cos(Θ)=0.5
cos(Θ)=0.8
dσ/dp_T dΩ*10^9(mb/GeV)
p_T(GeV/c)
5 15 25 35 45
0.4 0.8 1.2 1.6 2. 2.4 2.8
p̄p± → W^+ → l^++X, √s= 540 GeV
- - - h_p=+1 —— h_p=−1

Fig. 2a

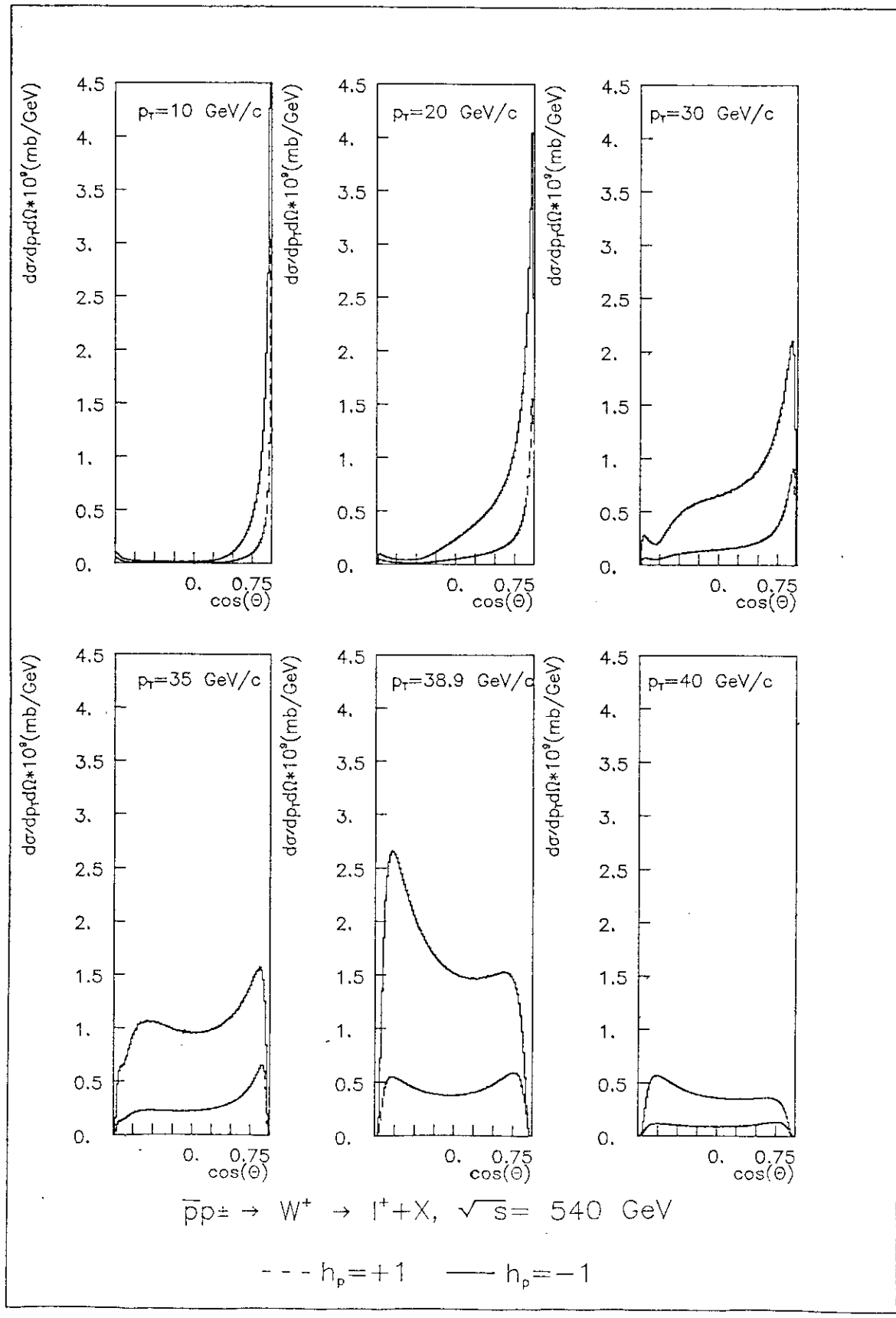
p_T=10 GeV/c
p_T=20 GeV/c
p_T=30 GeV/c
p_T=35 GeV/c
p_T=38.9 GeV/c
p_T=40 GeV/c
$d\sigma/dp_T d\Omega * 10^9$(mb/GeV)
cos(Θ)
$\bar{p}p^{\pm} \rightarrow W^{+} \rightarrow l^{+}+X$, $\sqrt{s}$= 540 GeV
h_p=+1
h_p=−1

Fig. 2b

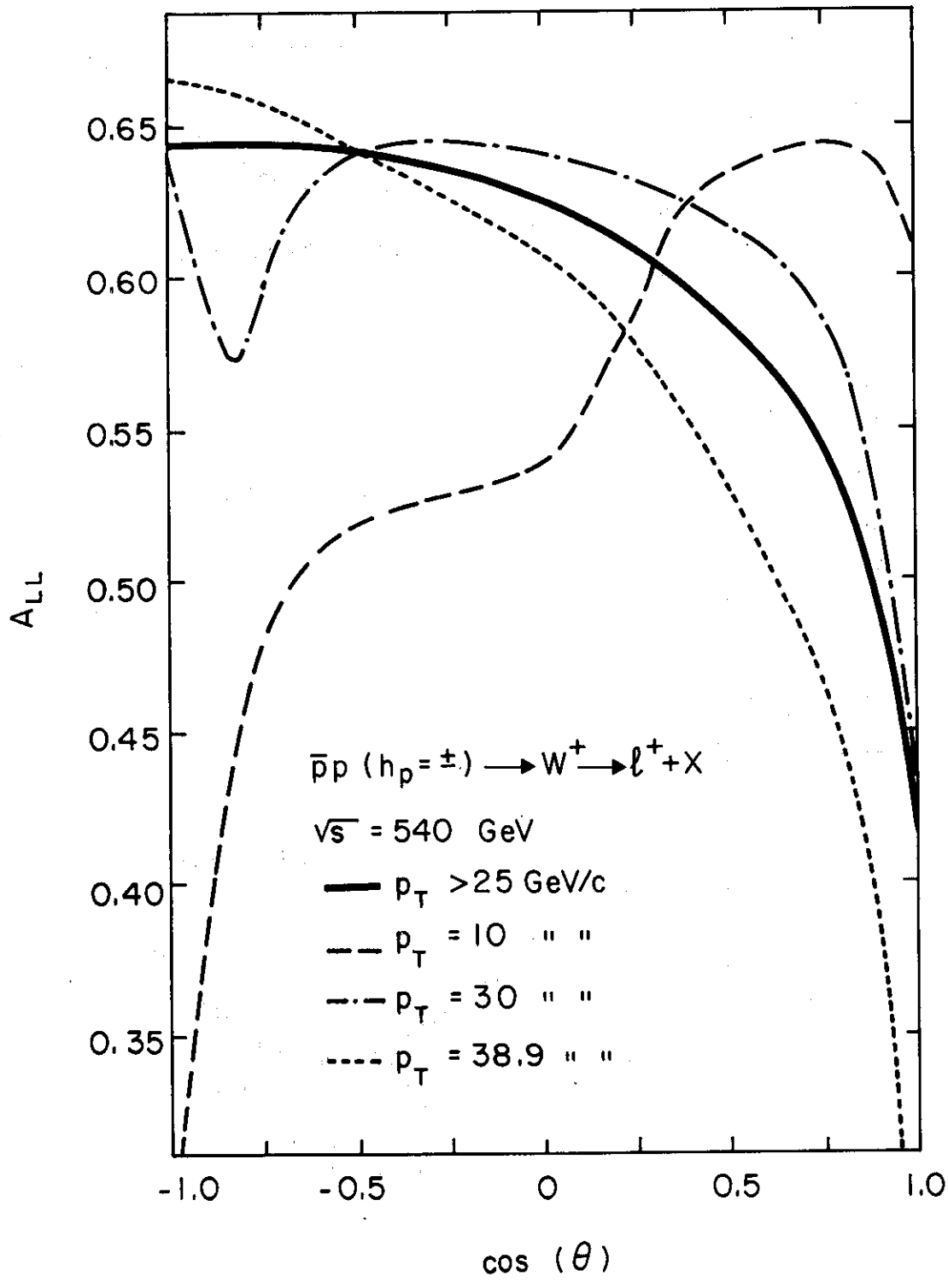
0.65
0.60
0.55
0.50
0.45
0.40
0.35
A_{LL}
$\bar{p}p\ (h_p = \pm) \longrightarrow W^+ \longrightarrow \ell^+ + X$
$\sqrt{s}$ = 540 GeV
p_T >25 GeV/c
p_T = 10 " "
p_T = 30 " "
p_T = 38.9 " "
-1.0
-0.5
0
0.5
1.0
cos (θ)

Fig. 3

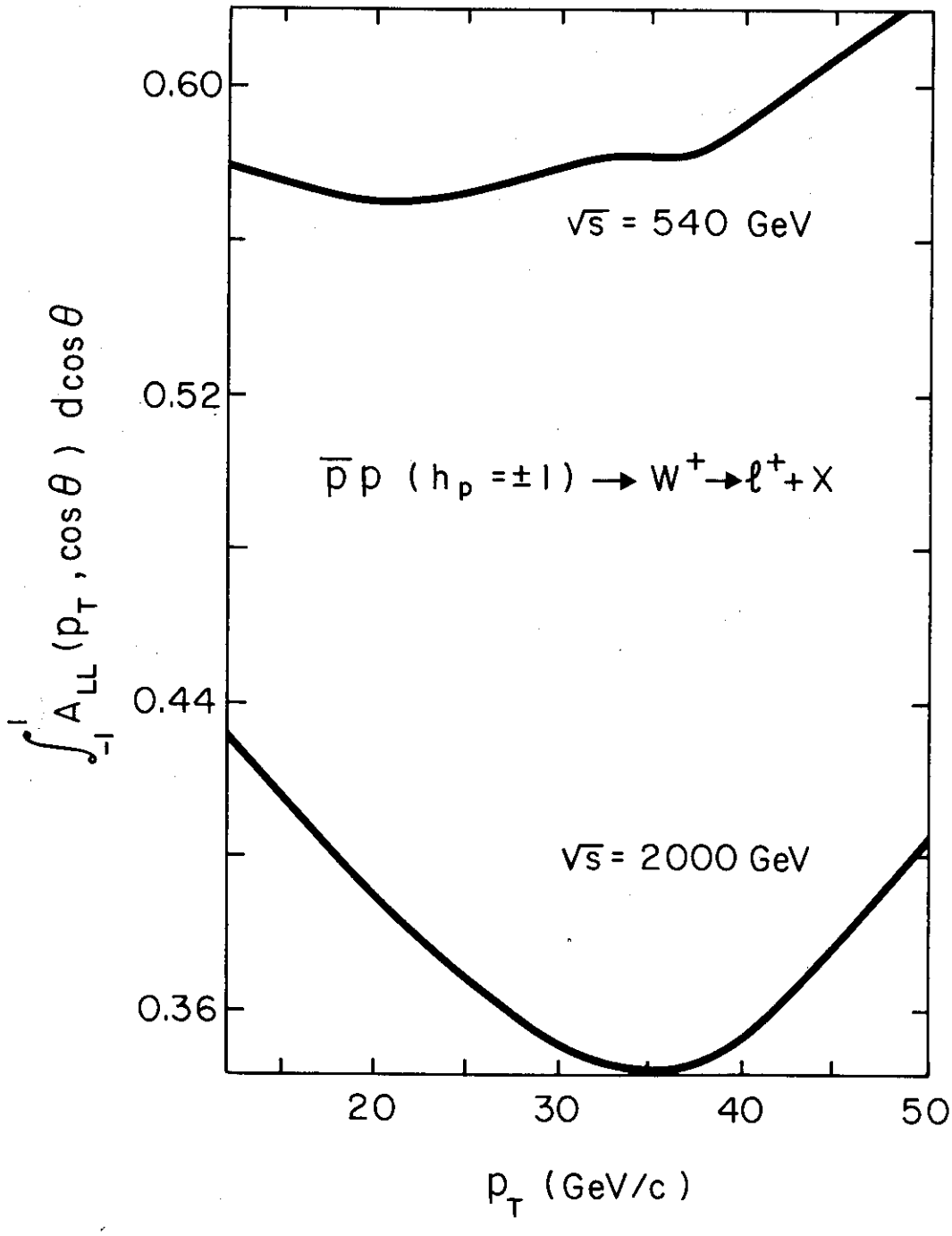
0.60
0.52
0.44
0.36
$\int_{-1}^{1} A_{LL}(p_T, \cos\theta)\, d\cos\theta$
$\sqrt{s}$ = 540 GeV
$\bar{p}p$ ($h_p = \pm 1$) → $W^+ \to \ell^+ + X$
$\sqrt{s}$ = 2000 GeV
20
30
40
50
p_T (GeV/c)

Fig. 4

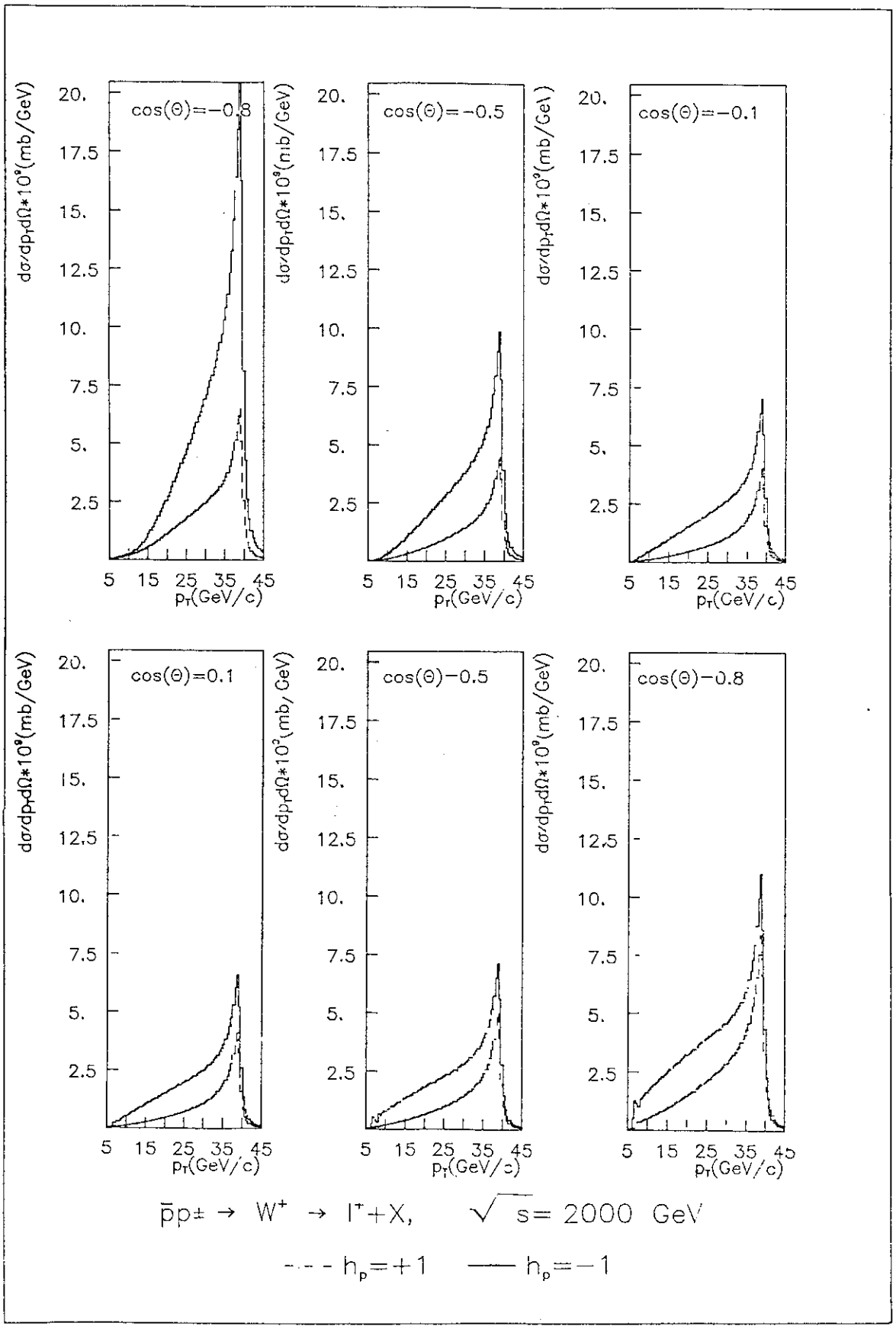
cos(Θ)=−0.8
cos(Θ)=−0.5
cos(Θ)=−0.1
cos(Θ)=0.1
cos(Θ)−0.5
cos(Θ)−0.8
dσ/dp_T dΩ*10⁹(mb/GeV)
dσ/dp_T dΩ*10⁹(nb/GeV)
dσ/dp_T dΩ*10³(mb/GeV)
p_T(GeV/c)
5 15 25 35 45
20. 17.5 15. 12.5 10. 7.5 5. 2.5
p̄p± → W⁺ → l⁺+X, √s= 2000 GeV
- - - h_p=+1 —— h_p=−1

Fig. 5a

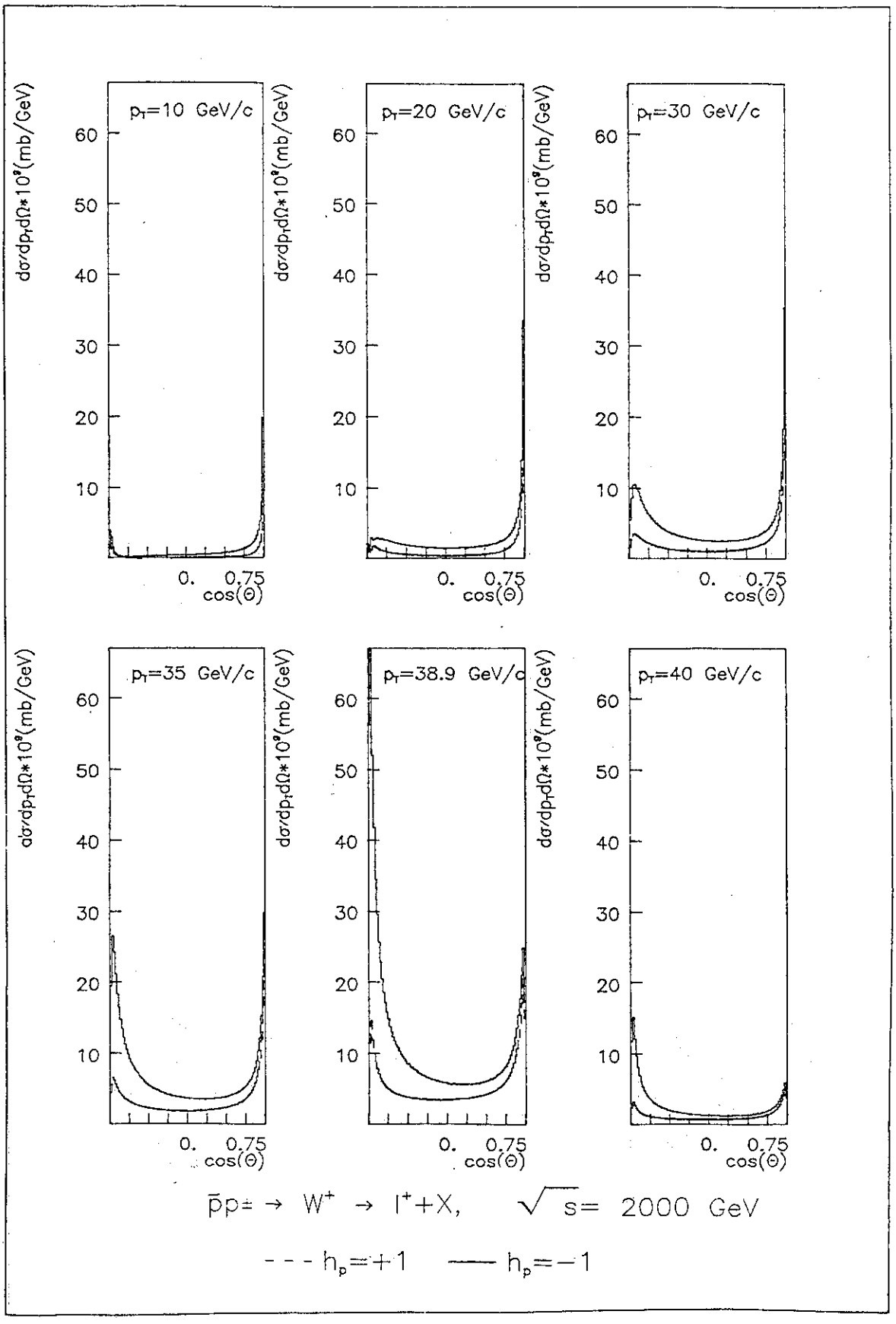
p_T=10 GeV/c
p_T=20 GeV/c
p_T=30 GeV/c
p_T=35 GeV/c
p_T=38.9 GeV/c
p_T=40 GeV/c
$d\sigma/dp_T d\Omega * 10^9$(mb/GeV)
60
50
40
30
20
10
0.
0.75
cos(Θ)
$\bar{p}p \rightarrow W^+ \rightarrow l^+ + X$, $\sqrt{s}$= 2000 GeV
--- h_p=+1
—— h_p=−1

Fig. 5b

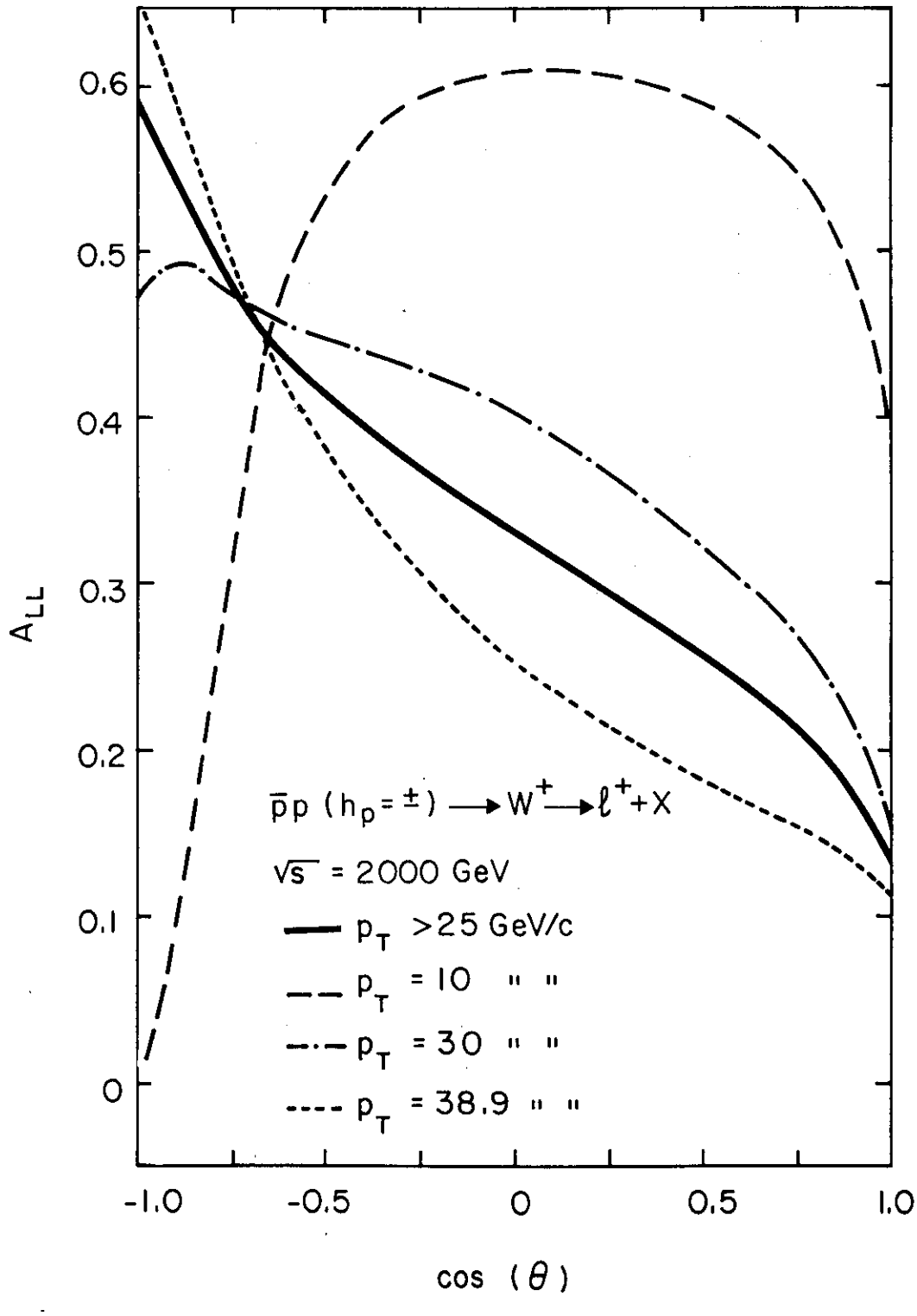
0.6
0.5
0.4
0.3
0.2
0.1
0
A_{LL}
$\bar{p}p\ (h_p = \pm) \longrightarrow W^+ \longrightarrow \ell^+ + X$
$\sqrt{s}$ = 2000 GeV
p_T >25 GeV/c
p_T = 10 " "
p_T = 30 " "
p_T = 38.9 " "
-1.0
-0.5
0
0.5
1.0
cos (θ)

Fig. 6

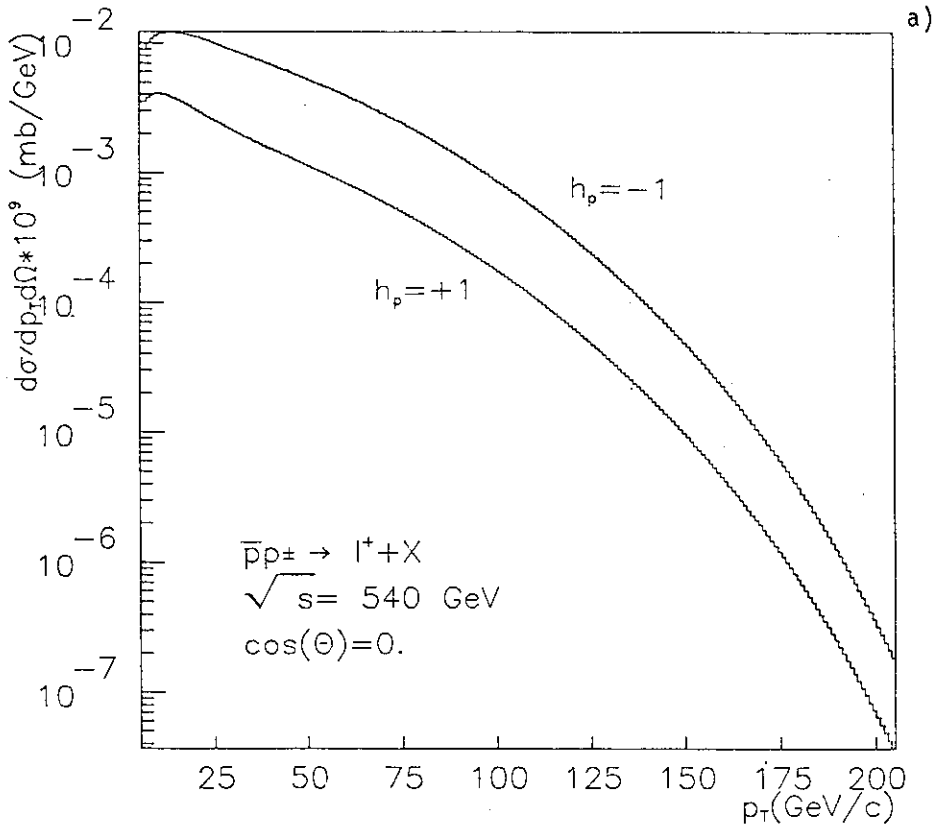
a)
$d\sigma/dp_T d\Omega * 10^9$ (mb/GeV)
10^{-2}
10^{-3}
10^{-4}
10^{-5}
10^{-6}
10^{-7}
$h_p=-1$
$h_p=+1$
$\bar{p}p^{\pm} \rightarrow l^+ + X$
$\sqrt{s}$= 540 GeV
cos(Θ)=0.
25 50 75 100 125 150 175 200
p_T(GeV/c)

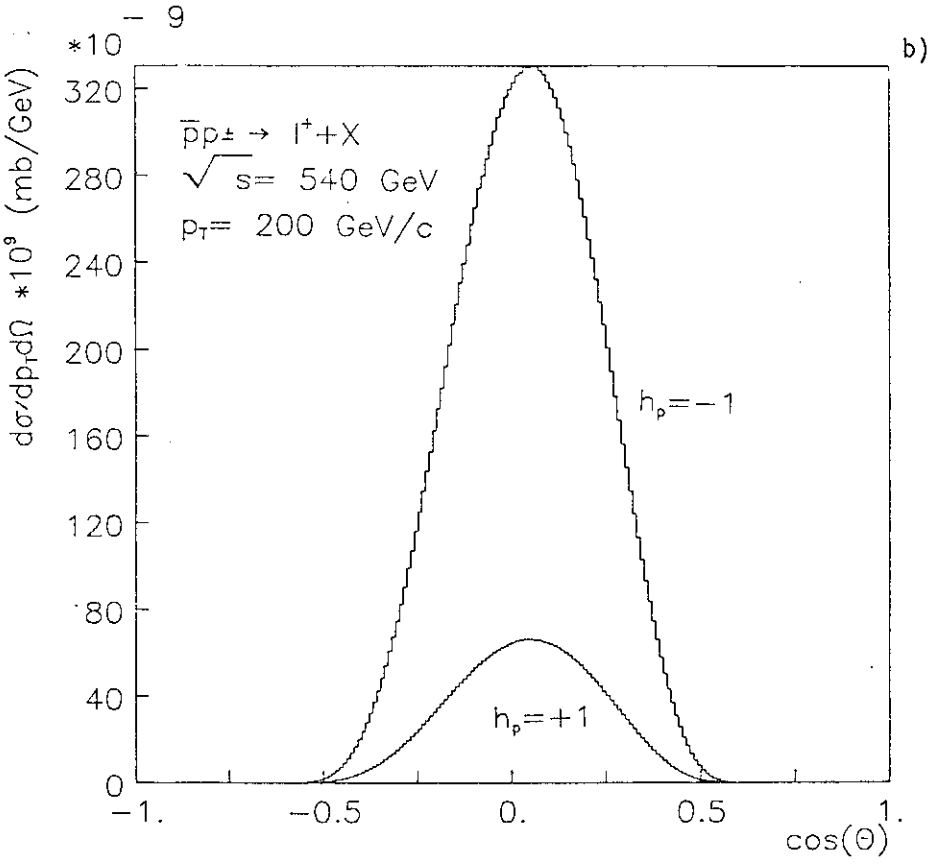
b)
$*10^{-9}$
$d\sigma/dp_T d\Omega * 10^9$ (mb/GeV)
320
280
240
200
160
120
80
40
0
$\bar{p}p^{\pm} \rightarrow l^+ + X$
$\sqrt{s}$= 540 GeV
p_T= 200 GeV/c
$h_p=-1$
$h_p=+1$
−1. −0.5 0. 0.5 1.
cos(Θ)

Fig. 7

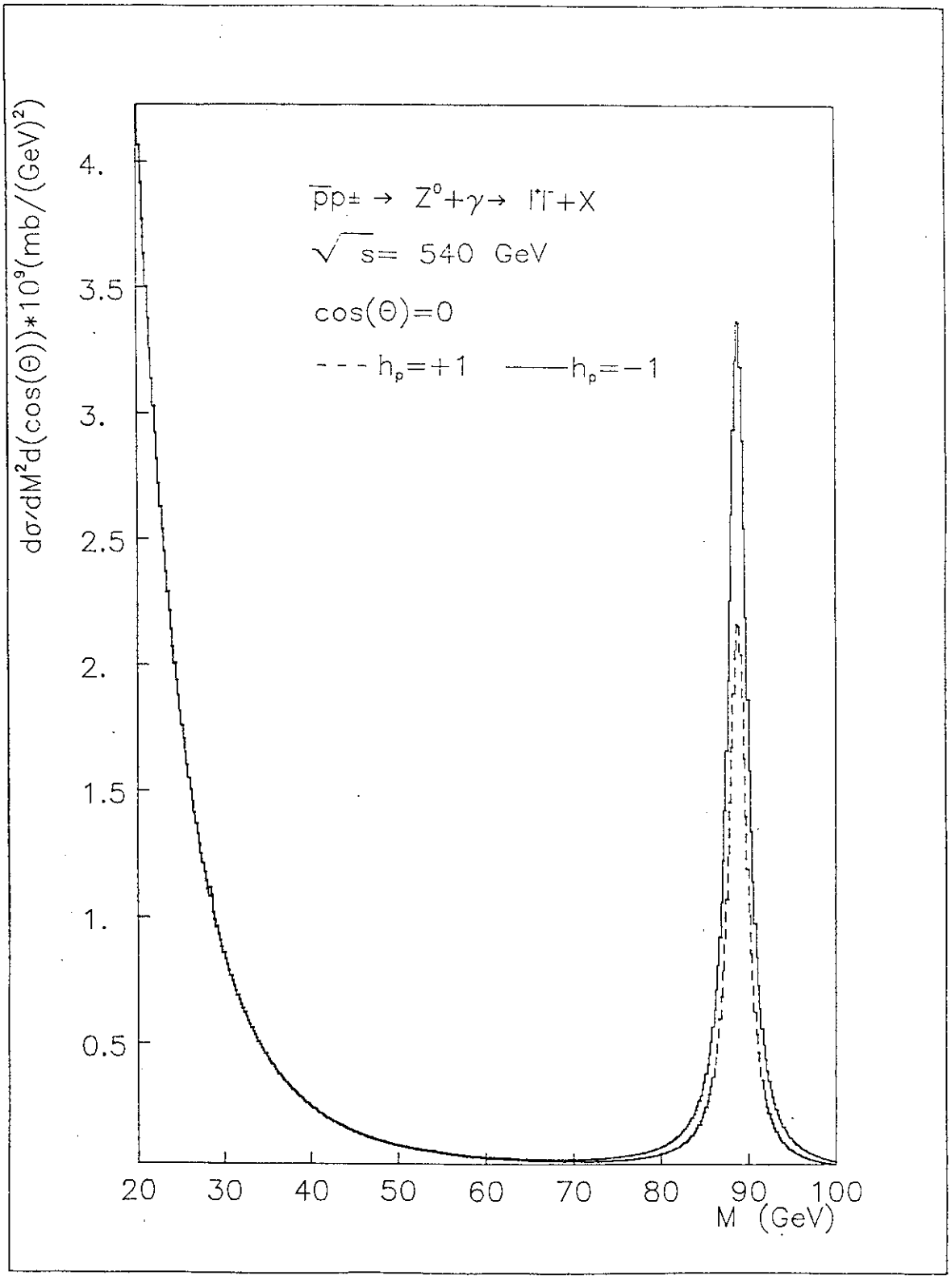
$d\sigma/dM^2d(\cos(\Theta))*10^9(mb/(GeV)^2)$
$\bar{p}p^{\pm} \rightarrow Z^0+\gamma \rightarrow l^+l^-+X$
$\sqrt{s} = 540$ GeV
$\cos(\Theta)=0$
$h_p=+1$
$h_p=-1$
4.
3.5
3.
2.5
2.
1.5
1.
0.5
20
30
40
50
60
70
80
90
100
M (GeV)

Fig. 8

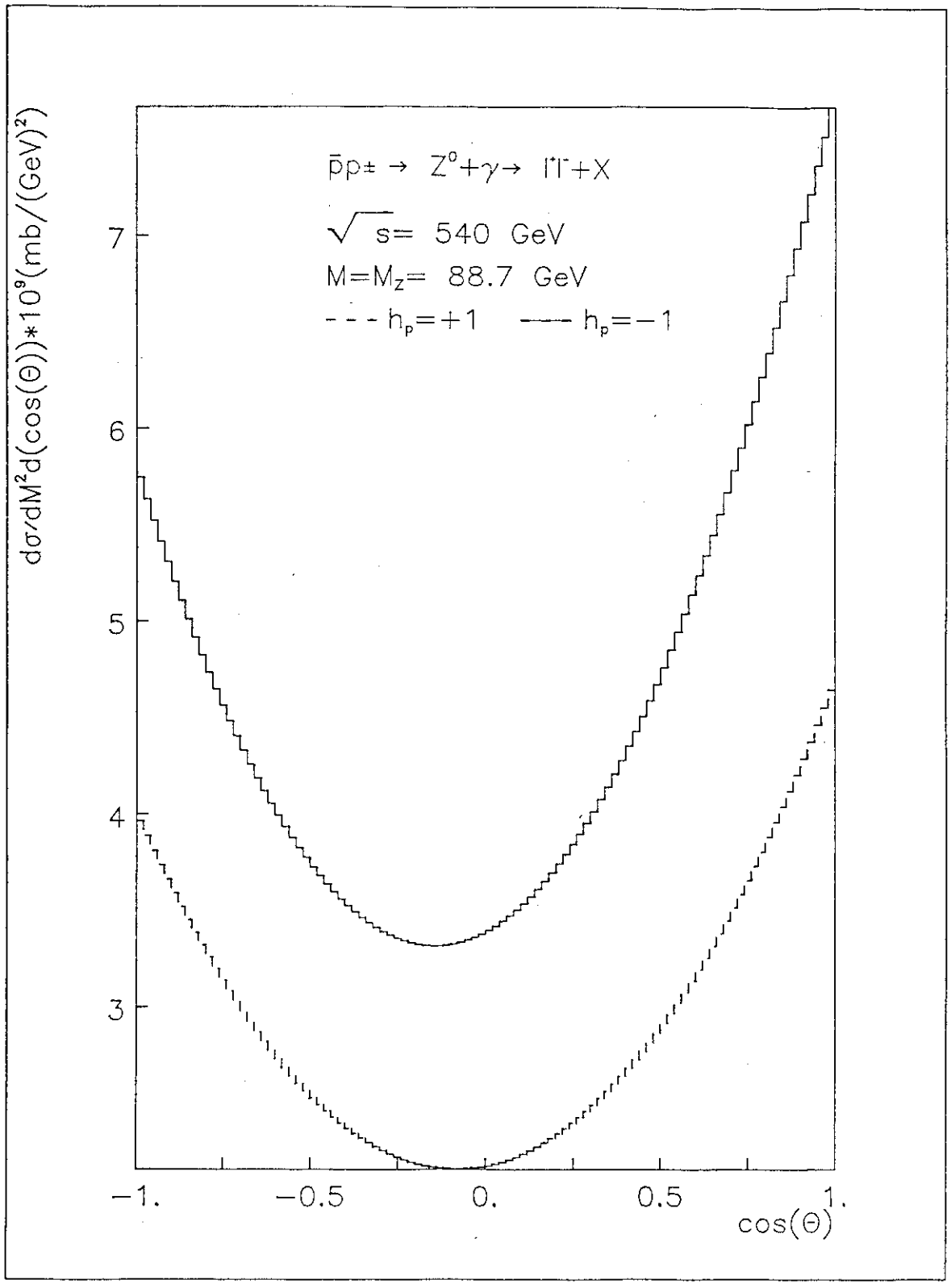
$\bar{p}p^{\pm} \rightarrow Z^0+\gamma \rightarrow l^+l^-+X$
$\sqrt{s}$= 540 GeV
M=M_Z= 88.7 GeV
--- h_p=+1 —— h_p=−1
$d\sigma/dM^2d(\cos(\Theta))*10^9$(mb/(GeV)^2)
7
6
5
4
3
−1.
−0.5
0.
0.5
1.
cos(Θ)

Fig. 9

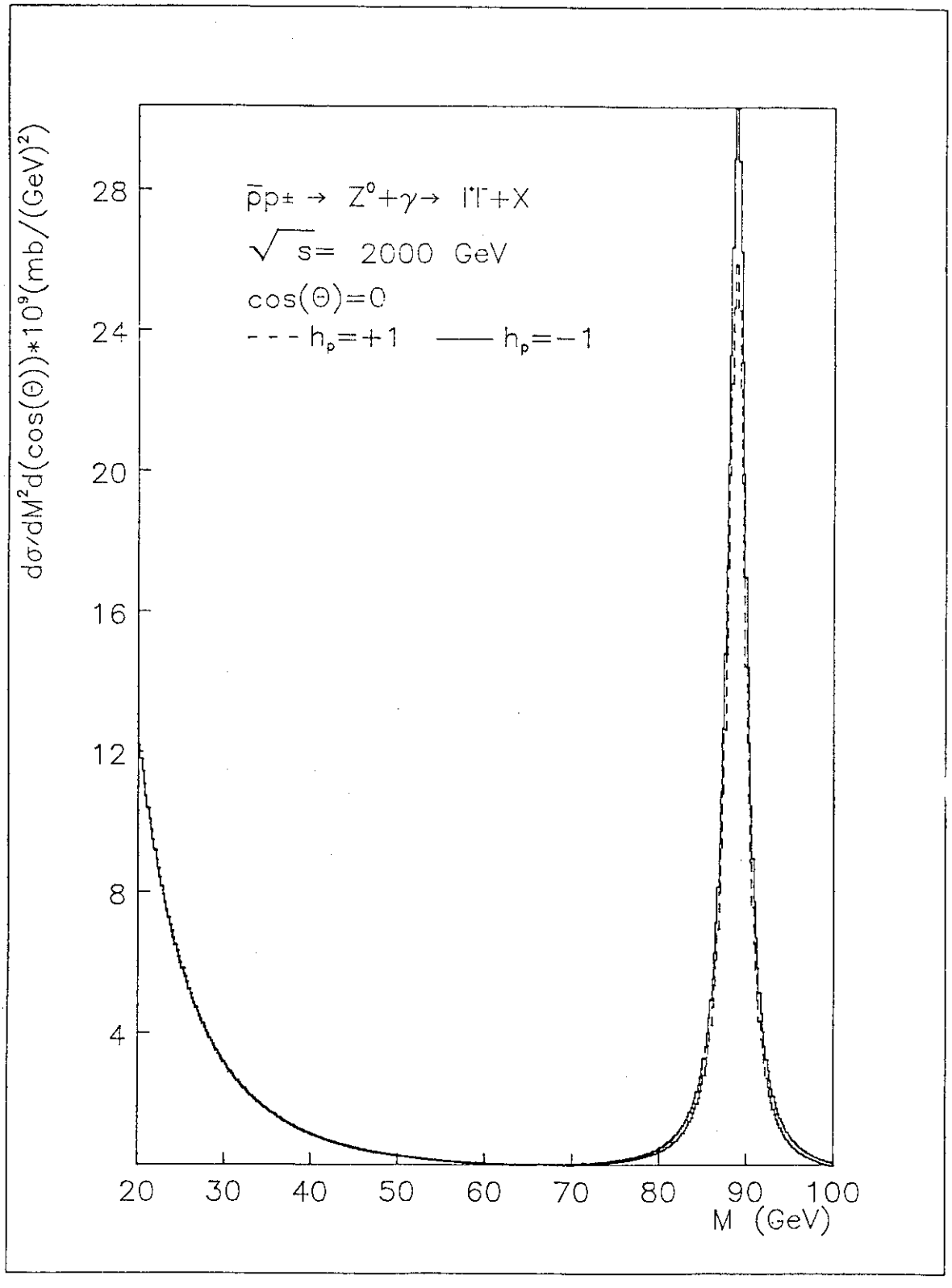
$d\sigma/dM^2d(\cos(\Theta))*10^9(mb/(GeV)^2)$
$\bar{p}p^{\pm} \rightarrow Z^0+\gamma \rightarrow l^+l^-+X$
$\sqrt{s}$= 2000 GeV
cos(Θ)=0
- - - h_p=+1 —— h_p=−1
28
24
20
16
12
8
4
20
30
40
50
60
70
80
90
100
M (GeV)

Fig. 10

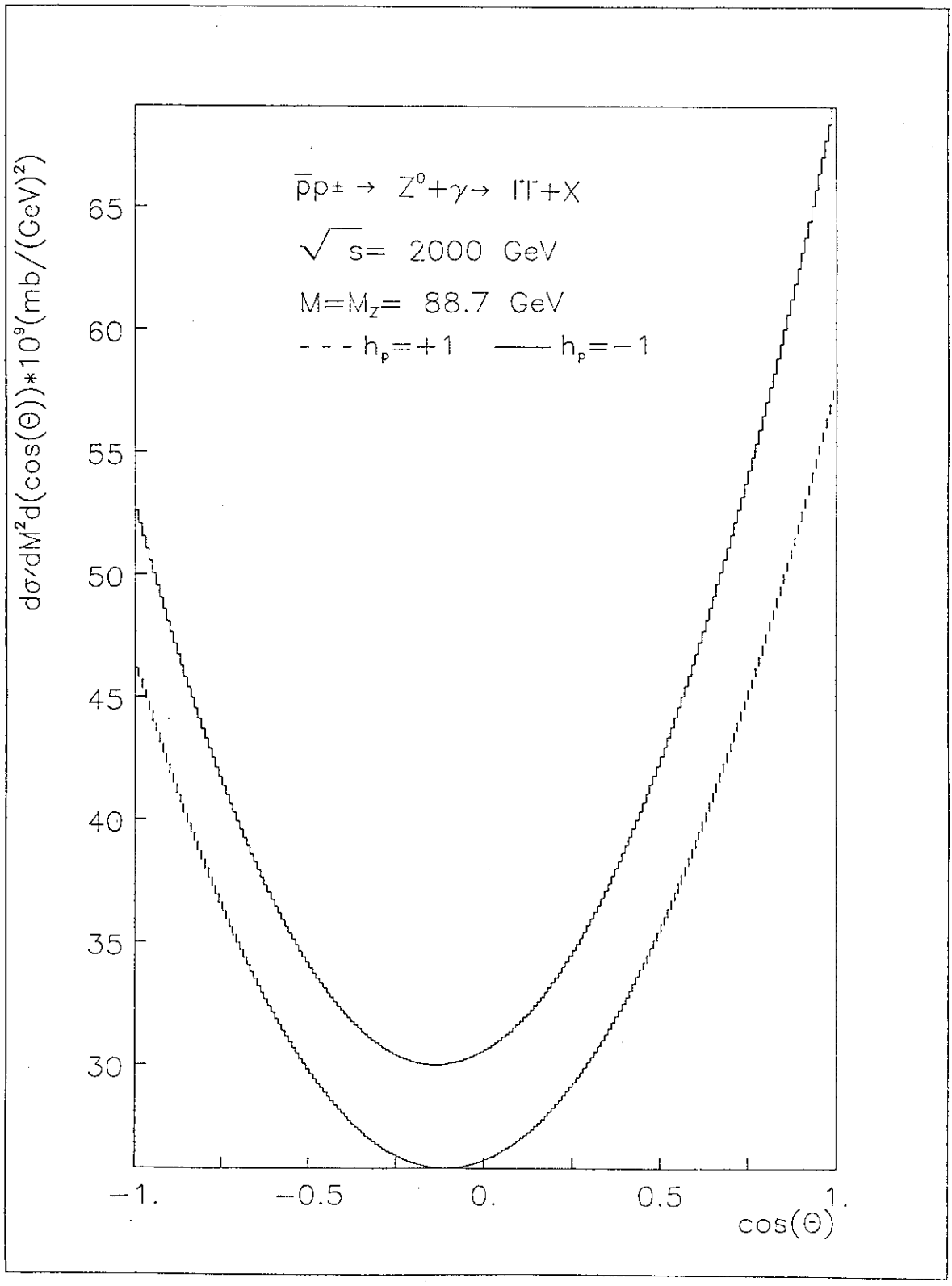
$\bar{p}p^{\pm} \rightarrow Z^0+\gamma \rightarrow l^+l^-+X$
$\sqrt{s}$= 2000 GeV
M=M_Z= 88.7 GeV
- - - h_p=+1 —— h_p=−1
$d\sigma/dM^2d(\cos(\Theta))*10^9$(mb/(GeV)^2)
65
60
55
50
45
40
35
30
−1.
−0.5
0.
0.5
1.
cos(Θ)

Fig. 11

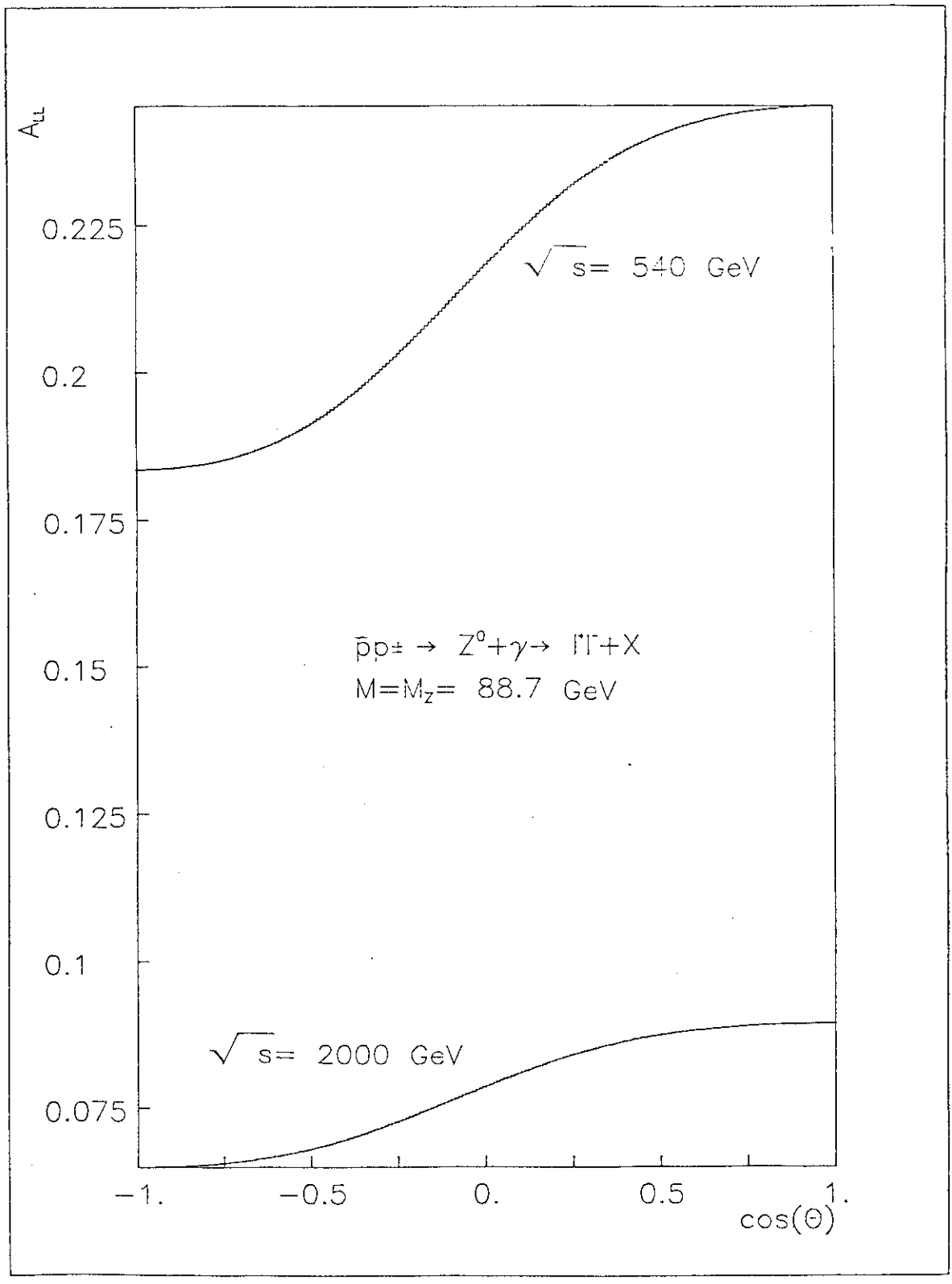
A_{LL}
0.225
0.2
0.175
0.15
0.125
0.1
0.075
$\sqrt{s}$= 540 GeV
$\bar{p}p^{\pm} \rightarrow Z^0+\gamma \rightarrow l^+l^-+X$
$M=M_Z$= 88.7 GeV
$\sqrt{s}$= 2000 GeV
−1.
−0.5
0.
0.5
1.
cos(Θ)

Fig. 12